Mathematical modeling of a solar powered humidification dehumidification desalination prototype

Reza Enayatollahi[1], Timothy Anderson[1], Roy Nates[1]

[1] Department of Mechanical Engineering, Auckland University of Technology, Auckland, New Zealand

renayato@aut.ac.nz

Abstract

In recent times the issue of fresh water shortages and salinity contamination of existing water sources has become a serious problem in a number of locations around the world. Hence, developing an environmentally friendly desalination technique is essential. In this work a theoretical model is developed in order to optimize a novel humidification-dehumidification desalination system. A sensitivity analysis was carried out, in order to find the optimum values for air and water flow rates. From this analysis it was found that a maximum of production rate of 1.5 kg/hr.m^2 was achievable, however it was also found that this rate was particularly influenced by the incident radiation, the inlet water temperature and the water flow rate.

Keywords: Humidification, Dehumidification, HDH, Desalination

1. Introduction

Fresh water demand is increasing considerably with population growth and improvement of living standards. Currently more than half of world's population is suffering from fresh water shortages [1]. Although nearly three-quarters of earth's surface is covered with water, only 3% of this water is potable [2] that is to say, it contains less than 500 ppm of salt [3]. Many current desalination plants use fossil fuels as the source of energy, but these are costly and not environmentally friendly [4]. Therefore, a large number of investigations have been aimed at finding efficient and clean techniques for water refinement [5,6,7,8,9]. Solar energy has the potential to solve these problems.

One of the cheapest and simplest ways to produce drinkable water is through the use of the Humidification Dehumidification (HDH) technique [10,11]. The HDH Desalination is a low temperature process often used to produce small amounts of desalted water [2]. Therefore it has the capability of using solar energy to drive it. The challenges for these systems are to minimize their size and complexity. Al-Hallaj et al, [10] designed and assessed a HDH Desalination unit with an open-air cycle and a capacity of 12 liter/day.m^2 of solar absorber area. It was reported that for this system that there was an optimum airflow rate, above and below which the fresh water production rate was reduced.

Zamen et al, [12] carried out an experimental investigation on a two-stage desalination unit with 80m^2 of solar panels. According to their report, productivity of the entire unit could be increased by 20% when compared with a single stage unit. It was also observed that using a two-stage method could increase heat

recovery in the condenser and consequently decrease the size of the thermal energy system per unit of fresh water produced.

Bacha et al, [13] conducted a mathematical and experimental study on a HDH Desalination unit in which both water and air heating techniques were applied. According to their work the two-temperature mathematical model better describes the real behavior of the water collector compared to the one-temperature model.

Given the potential for HDH desalination, the aim of this work is to develop a generalized design model to aid the development of such systems and predict their performance and optimal operating conditions.

2. System Description

The present study is based on the open air-closed water HDH cycle, for a small household, as shown in Figure 1.

For the proposed system a double-glazed flat plate solar collector with an absorber area of 2 m^2 is used for heating the saline water. The water from a very large reservoir, which is fed by the preheated water from the condenser together with make-up water from the saline source, enters the collector where it is heated, providing the required heat for evaporation, before exiting into the evaporator. The evaporator acts as the humidifier and is of a cascading design. In doing this, it utilizes a counter-current flow arrangement with ambient air introduced into the system.

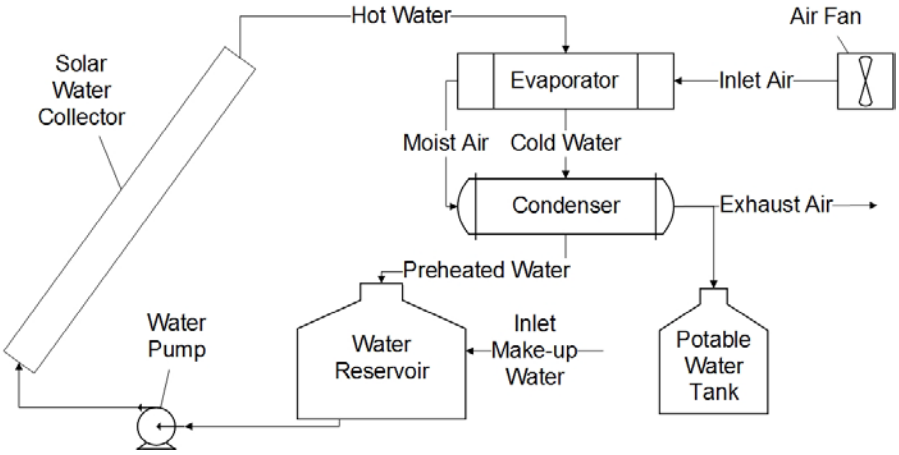

Figure 1. HDH Desalination Unit

As a result of the contact between the heated water and the air, some water will be evaporated, ideally saturating the air. This evaporation will cause a temperature drop in the remaining water, and if the evaporation area is large enough relative to the water flow rate, the outgoing water from the evaporator can be used as the cooling fluid in the condenser. This cooled water exiting the evaporator, enters the condenser, which consists of a shell and tube heat exchanger. Cold water from the evaporator enters on the shell side and hot moist air enters the tubes. As a result of heat transfer between these two streams

water vapor in the air will be condensed, thus delivering potable water. The design parameters for the proposed system are shown in Table 1.

Table 1. Design Parameters

Water collector		Evaporator		Condenser		Ambient Condition	
$T_{w,in,col}$	293.2 [K]	$T_{a,in,sys}$	294.2 [K]	$N_{tube,cond}$	20	$Rh_{a,amb}$	60 [%]
$\dot{V}_{w,in,col}$	$1.17*10^{-5}$ [m^3/s]	$\dot{V}_{a,in,sys}$	0.017 [m^3/s]	L_{cond}	2 [m]	s	38 [°]
$N_{tube,col}$	20	$N_{Tray,evap}$	29	$N_{baffle,cond}$	19	G_t	1000 [W/m^2]
$D_{o,tube,col}$	0.0127 [mm]	L_{evap}	2 [m]	$D_{o,tube,cond}$	0.0127 [mm]	P_{sys}	101.325 [kpa]
$D_{i,tube,col}$	0.01181 [mm]	W_{evap}	1 [m]	$D_{i,tube,cond}$	0.01181 [mm]	V_{wind}	5 [m/s]
$N_{glass,col}$	1	D_{evap}	0.4 [m]	$D_{shell,cond}$	0.2129 [m]	R_v	0.4615 [kJ/kg.K]

The water reservoir is considered sufficiently large so that the inlet water temperature can be assumed constant. It is decided that the power required for the fan and pump would not be a concern of this investigation, but would be provided by an auxiliary PV system.

3. Method

As mentioned earlier a standard double-glazed, flat plate solar collector is designed in order to heat up the water before entering the evaporator. The outlet water temperature from the collector can be calculated from Equation 1.

$$T_{w,out,col} = T_{w,in,col} + \frac{Q_{u,col}}{\dot{m}_{w,in,col} cp_{w,col}} \quad (1)$$

In which, $cp_{w,col}$, $\dot{m}_{w,in,col}$ and $T_{w,in,col}$ are the specific heat, mass flow rate and temperature of inlet water to the collector, respectively. $Q_{u,col}$ represents the useful energy gained by water and it is determined by solving the following Equations 2 and 3, simultaneously.

$$Q_{u,col} = A_{col}[G_a - U_{col}(T_{p,col} - T_{amb})] \quad (2)$$

$$T_{p,col} = T_{w,in,col} + \frac{Q_{u,col}/A_{col}}{U_{col} F_{R.col}}(1 - F_{R,col}) \quad (3)$$

where, U_{col} is the collector overall heat loss coefficient $T_{p,col}$ is the absorber plate temperature, A_{col} is the collector area, G_a is the absorbed radiation, T_{amb} is the ambient temperature and $F_{R,col}$ is the heat removal factor calculated by Equation 4.

$$F_{R,col} = \frac{\dot{m}_{w,in,col} cp_{w,col}}{A_{col} U_{col}} \left[1 - e^{\frac{-A_{col} U_{col} F'_{col}}{\dot{m}_{w,in,col} cp_{w,col}}}\right] \quad (4)$$

In Equation (4), F'_{col} is the collector efficiency factor defined by Equation 5.

$$F'_{col} = \frac{1/U_{col}}{w\left[\frac{1}{U_{col}\left(2L_s F + D_{o,tube,col}\right)} + \frac{1}{C_B} + \frac{1}{h_{i,tube,col}\pi D_{i,tube,col}}\right]} \quad (5)$$

Where, w is tube spacing, C_B is the bond conductance, L_s is the tube pitch, F is the fin efficiency given by Equation 6 and $h_{i,tube,col}$ is the heat transfer coefficient of water inside the collector's tubes. Finally, $D_{i,tube,col}$ and $D_{o,tube,col}$ are the inner and outer diameters of the collectors tubes, respectively.

$$F = \frac{1}{mL_s}\left[\frac{\exp(mL_s) - \exp(-mL_s)}{\exp(mL_s) + \exp(-mL_s)}\right] \quad (6)$$

Where,

$$m = \sqrt{U_{col}/k_p l_p}$$

where, k_p and l_p are thermal conductivity and thickness of absorber plate.

The collector overall heat loss coefficient U_{col} is the summation of bottom, edge and top heat loss coefficients. Bottom and edge heat loss coefficient can be calculated from equations 7 and 8, respectively.

$$U_{bottom} = \frac{k_{ins}}{l_{ins}} \quad (7)$$

$$U_{edge} = U'_{edge}\left(\frac{A_{perimeter}}{A_{col}}\right) \quad (8)$$

In which, k_{ins} and l_{ins} are the thermal conductivity and thickness of insulation. U'_{edge} is the edge overall loss coefficient and was assumed to be 0.5 for design purposes, and $A_{perimeter}$ is the edge area. In order to calculate the top loss coefficient, Equation 9 can be used [14].

$$U_{top} = \left[\frac{N_{g,col}}{\frac{G}{T_{p,col}}\left(\frac{T_{p,col} - T_{amb}}{N_{g,col} + B}\right)^{0.33}} + \frac{1}{h_{wind}}\right]^{-1} + \frac{\sigma\left(T_{p,col} + T_{amb}\right)\left({T_{p,col}}^2 + {T_{amb}}^2\right)}{\left[\varepsilon_{p,col} + 0.5N_{g,col}\left(1 - \varepsilon_{p,col}\right)\right]^{-1} + \frac{2N_{g,col} + B - 1}{\varepsilon_{g,col}} - N_{g,col}} \quad (9)$$

where $N_{g,col}$ is the number of glass covers, G is the total radiation, B and Z are empirical variables, σ is the Stephan-Boltzman constant and $\varepsilon_{p,col}$ and $\varepsilon_{g,col}$ are emissivity of absorber plate and glass cover.

$$Z = 250[1 - 0.0044(s - 90)]$$

$$B = \left[1 - 0.04h_{wind} + 0.0005{h_{wind}}^2\right][1 + 0.091N_{g,col}]$$

Where h_{wind} is wind heat transfer coefficient and s is the slope of water collector.

The evaporator is modeled considering the counter-current flow pattern for water and air streams. In fact the evaporator is a simultaneous heat and mass exchanger that takes the air from the atmosphere and water from the solar collector. Therefore, for a given water flow rate, if the evaporation area is large enough, it can be used as a water chiller at the same time.

Considering, that the mass flow rate of air ($\dot{m}_{a,evap}$) is constant, Equations 10 and 11 give the energy and mass balance on the evaporator.

$$\dot{m}_{a,evap}(h_{a,in,evap-}h_{a,out,evap}) + \dot{m}_{w,in,col}h_{w,in,evap} = \dot{m}_v h_v + \dot{m}_{w,out,evap}h_{w,out,evap} \quad (10)$$

where, h_v is the enthalpy of vaporization at the film temperature, $\dot{m}_v$ is the rate of evaporation, $h_{a,in,evap}$ and $h_{a,out,evap}$ are the enthalpies of air at inlet and outlet of the evaporator and $h_{w,in,evap}$ and $h_{w,out,evap}$ are the enthalpies of water at inlet and outlet of the evaporator. Mass flow rates of water at the outlet of the evaporator can be calculated from equation 11.

$$\dot{m}_{w,out,evap} = \dot{m}_{w,in,col} - \dot{m}_v \quad (11)$$

In which the rate of evaporation can be computed from Equation 12 [15].

$$\dot{m}_v = J_{mass}\frac{A_{evap}}{R_v}\left[\frac{P_{sat,f}}{T_f} - \frac{P_{sat,evap}}{T_{a,evap}}\right] \quad (12)$$

where, J_{mass} is the mass transfer coefficient, being a function of the Sherwood number [16], and R_v is the gas constant for water vapor. A_{evap} represents the total evaporation area, T_f and $T_{a,evap}$ are the film and air temperatures. $P_{sat,f}$ is the saturation pressure at film temperature and $P_{sat,evap}$ is the saturation pressure at the air temperature.

This system is analogous to a counter-current heat exchanger with phase change and can be solved by applying the Number of Transfer Units (NTU) method. However, using the NTU method ignores the effect of vaporization in the collector due to the assumption of no mass transfer between air and water streams. In order to take the effect of vaporization into account, the total required heat of evaporation must be considered. Since the evaporator is well-insulated the required heat of evaporation comes from the water and air stream determined with respect to their specific heats. This results in lower enthalpies of water and air streams than would be calculated with the NTU method alone. The energy and mass balance given in Equations10 and 11 is used to correct this.

Subsequently Equations 13 and 14 can be used to estimate the outlet temperatures of the air and water [17].

$$T_{a,out,evap} = T_{amb} + \frac{\dot{Q}_{NTU}}{\dot{m}_{a,in,evap}cp_{a,in,evap}} \quad (13)$$

$$T_{w,out,evap} = T_{w,out,col} - \frac{\dot{Q}_{NTU}}{\dot{m}_{w,in,evap}cp_{w,in,evap}} \quad (14)$$

where, $cp_{a,in,evap}$ represents the specific heat of air at the evaporator inlet and $\dot{Q}_{NTU}$is the product of the effectiveness and maximum possible energy gain, as shown in Equation 15.

$$\dot{Q}_{NTU} = E\dot{Q}_{Max} \quad (15)$$

Where Equation 16 is used to determine the maximum possible energy gained and Equation 17 defines the Effectiveness.

$$\dot{Q}_{Max} = \dot{m}cp_{min}(T_{w,out,col} - T_{amb}) \quad (16)$$

in which $\dot{m}cp_{min}$ is the minimum product of the mass flow rate and specific heat of the air or water stream.

$$E = 1 - \exp(-NTU) \quad (17)$$

And where Equation 18 gives the NTU.

$$NTU = \frac{U_{evap}A_{evap}}{\dot{m}cp_{min}} \quad (18)$$

And where, U_{evap} is the evaporator overall heat transfer coefficient.

$$U_{evap} = \frac{1}{\frac{1}{h_a}+\frac{1}{h_w}}$$

In the above equation h_a and h_w are the heat transfer coefficient of air and water respectively.

A single pass shell and tube heat exchanger is to be used as the dehumidifier. Therefore, the NTU method used for evaporator can be used for the condenser as well. However, in the evaporator there is no splitting layer between cooling and heating fluid, while in the condenser they are separated by means of condenser tubes. Hence, heat transfer coefficients in each of the pipes must be considered in the calculation of overall heat transfer coefficient. Equation 19 is given to calculate the overall heat transfer coefficient of the condenser.

$$U_{cond} = \frac{1}{\frac{1}{h_a}+\frac{A_{i,tube}\ln\left[\frac{r_{o,tube}}{r_{i,tube}}\right]}{2\pi k_{tube}L_{tube}}+\frac{A_{i,tube}}{A_{o,tube}}\frac{1}{h_w}} \quad (19)$$

where, $A_{i,tube}$ and $A_{o,tube}$ are the inner and outer area of condenser's tubes. $r_{i,tube}$ and $r_{o,tube}$ are the inner and outer radius of each tube and finally, k_{tube} and L_{tube} are the thermal conductivity and length of tubes of the condenser respectively.

Finally the amount of potable water production is the difference between specific humidity of air at both ends of the condenser. Equation 20 is given to calculate the mass flow rate of potable water production.

$$\dot{m}_{potable} = \dot{m}_{a,out,evap}\Delta\omega_{cond} \quad (20)$$

where, $\Delta\omega_{cond}$ is the difference between specific humidity of air at inlet and outlet of the condenser.

4. Results

Based on the initial design conditions, introduced in Table 1, a sensitivity analysis was performed to determine the influence of the design parameters on the production rate of fresh waters.

In the first instance it was decided to examine the influence on radiation on the systems production rate. In Figure 2 it can be seen that increasing the radiation on the absorber increases the total production of potable water. This is

because increased radiation on the absorber plate results in greater energy gain by water and consequently a higher rate of evaporation. Further, it can be seen that there is a slight change in the slope of the production curve at around 1000 W/m^2; this is due to an increase in specific humidity of air at the condenser inlet leading to sensible heating above saturation conditions. Therefore, the air entering the condenser needs further cooling to approach the dew point temperature.

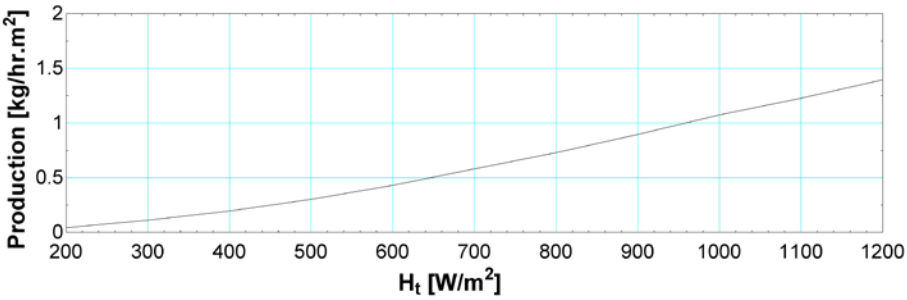

Figure 2. Production Rate of Potable water vs. Total Radiation

In Figure 3, the effect of changing inlet water temperature on potable water production is shown. By increasing the inlet water temperature to the collector the total input energy to the system is also increased, which results in more evaporation of water. Thus, as the graph shows increasing the inlet water temperature will increase the production rate, leading to a maximum yield of approximately 1.5 kg/hr.m^2.

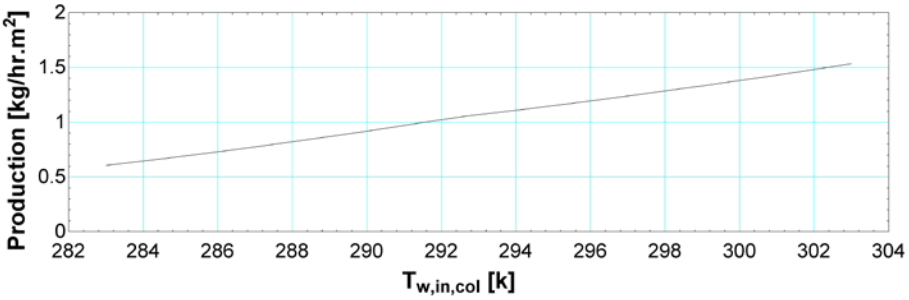

Figure 3. Production Rate of Potable Water vs. Inlet Water Temperature

In Figure 4 the effect of varying the air flow rate on the production rate can be seen. In this it can be seen that production rate initially increases with increasing air flow rate to an optimum value, and beyond that it decreases. This can be explained by the fact that increasing the air flow rate brings more energy to the system, but reduces the residence time in each heat exchanger. Consequently the air temperature at the evaporator outlet decreases with increasing the airflow rate and the outlet air temperature from the condenser increases. A reduction in air temperature at the evaporator's outlet leads to a reduction in specific humidity of air entering the condenser, and an increase in outlet air temperature from the condenser results in a higher specific humidity of air exiting the evaporator. Accordingly, the specific humidity difference at both ends of condenser, which drives the production, decreases.

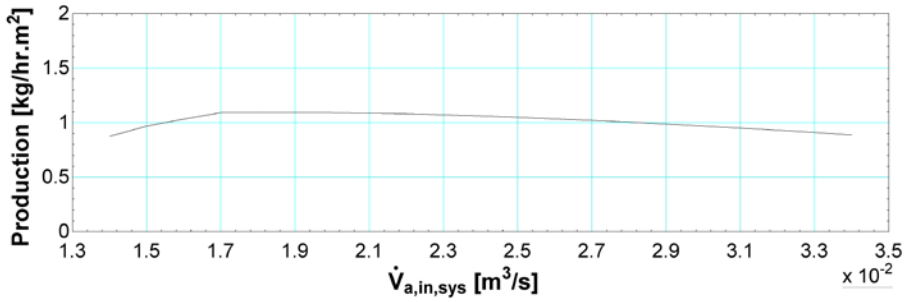

Figure 4. Production Rate of Potable Water vs. Volume Flow Rate of Air

Now, in Figure 5, it can be seen that increasing the water flow rate decreases the potable water production. This is because increasing the water flow rate decreases the water temperature at the evaporator's inlet, and thus its propensity to evaporate.

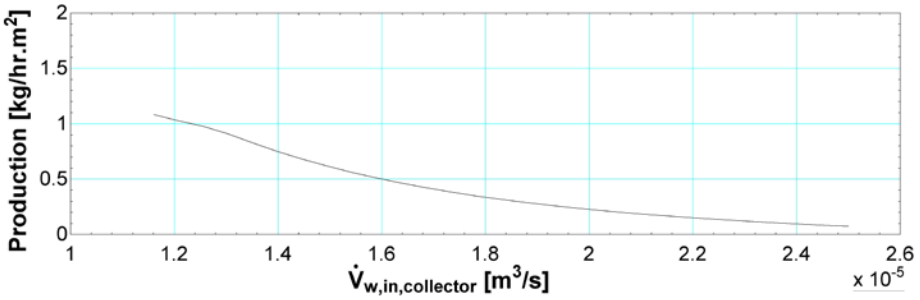

Figure 5. Production Rate of Potable Water vs. Volumetric Flow rate of Water

Unlike the water temperature, in Figure 6, it can be seen that increases in the ambient air temperature increase the potable water production up to an optimum value, and beyond that we observe a reduction in production. This is because increasing the inlet air temperature brings more energy to the system, this results in increasing the evaporation and consequently potable water production. However, ambient air is meant to cool down the inlet water to the condenser, hence, the difference between specific humidity of air at both ends of the condenser decreases due to the higher temperature of water at the condenser inlet.

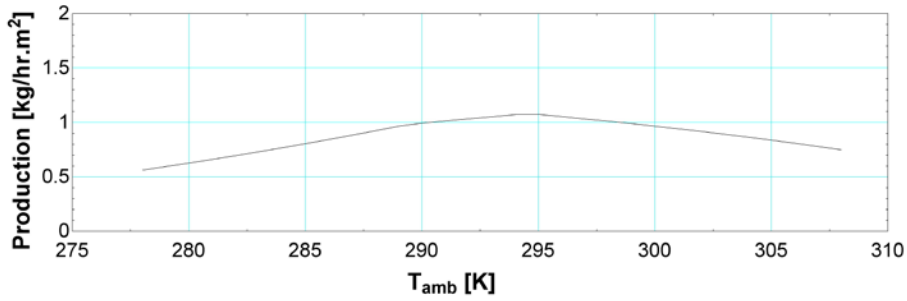

Figure 6. Production Rate of Potable Water vs. Ambient Air Temperature

Quite obviously one of the key design parameters for a HDH system is the evaporator and it would be reasonable to expect that increasing the evaporation area would allow more water to evaporate. However, the ability of moisture to be absorbed by air decreases as the relative humidity of air increases in the evaporator. Hence, as shown in Figure 7, increasing the evaporation area to 14.5 m^2 causes a marked increase in production and beyond that production rate increases only slightly suggesting that this is the maximum realistic evaporator size.

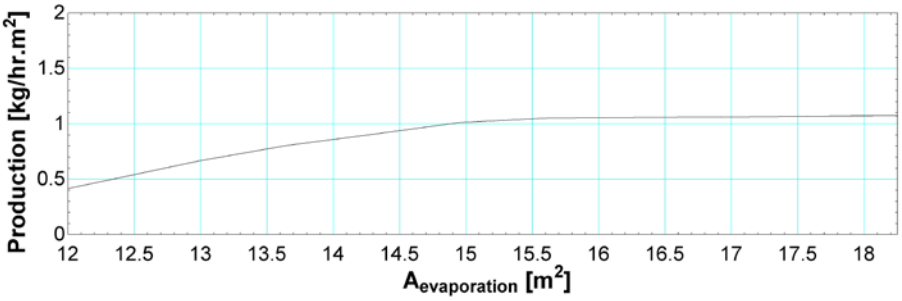

Figure 7. Total production of potable water vs. evaporation area

Conversely, providing larger condensation area allows more heat transfer between water and air streams. Therefore, it might be expected that higher production rates would occur with larger condensation areas. The condensation area could be increased either by increasing the length of tubes or number of them. However, increasing the number of tubes reduces the air velocity and consequently lowers the heat transfer coefficient. Therefore changing the number of tube has a smaller effect on production compare to influencing their length.

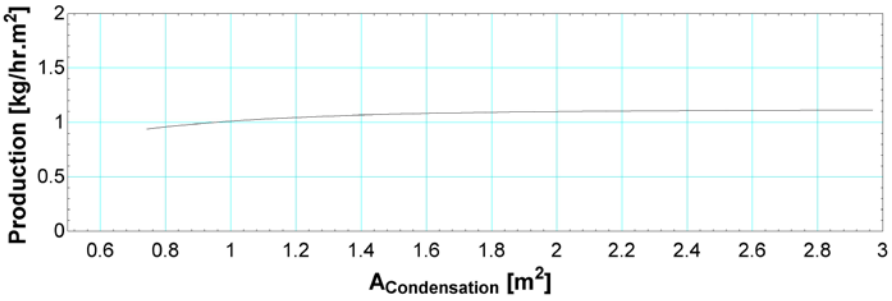

Figure 8. Total production of potable water vs. Condensation area

5. Conclusion

A solar desalination unit based on the humidification-dehumidification technique was modeled. The effect of changing the water and airflow rates in addition the evaporation and condensation area was studied. It was found that the designed system could have a capacity of up to 1.5 kg/hr.m^2 under ideal circumstances, however it was observed that the water production increased with increasing air flow rates to an optimum value beyond which it decreased. Additionally increasing the water flow rate resulted in decreasing the potable production. Finally, it was shown that evaporation and condensation area placed a constraint on the production rate at any given condition.

References

[1] El-Dessouky, Ettouney, H., Al-Juwayhei, "Analysis of single-effect evaporator desalination systems combined with vapor compression heat pumps ," Desalination, 114, 253-275, (1997).

[2] Ettouney, H., Fawzy, N., Al-Enzei, "Low temperature humidification dehumidification desalination process," Energy Conversion and Management, 47, 470-484, (2006).

[3] Banat, F., Qtaishat, M. R., "Desalinatyion by solar powered membrane distilation system," Desalination, 308, 186-197, (2012).

[4] Behzadmehr, A., Farsad, S., "Analysis of solar desalination unit with humidification dehumidification cycle using DoE method ," Desalination, 278, 70-76, (2011).

[5] Al-Tahaineh, H. A., Bardan, O. O., "The effect of coupling a flat-plate collector on the solar still productivity ," Desalination, 183, 137-142, (2005).

[6] Vinothkumar, K., Ahsan, A., Jayaprakash, R., Kumar, S., Arunkumar, T., "Experimental study on various solar still designs ," International Scholarly Research Network, 2012, (2012).

[8] McGovern, R. K., Zubair, S. M., Lienhard, J. H., Narayan, V. P., "High-temperature-steam-driven, varied-pressure, humidification-dehumidification system coupled with reverse osmosis for energy-efficient seawater desalination," Energy, 37, 482-493, (2011).

[7] Zhang, H., Yuan, G., "Mathematical modeling of a closed circulation solar desalination unit with humidification-dehumidification," Desalination, 205,156-162, (2006).

[9] Ben Bacha, H., Zhani, K., "Experimental investigation of a new solar desalination prototype using the humidification dehumidification principle ," Renewable Energy, 35, 2610-2617, (2010).

[10] Farid, M. M., Tamimi, A. R., Al-Hallaj, S., "Solar desalination with a humidificatiom-dehumidification desalination cycle: performance of the unit," Desalination, 120, 273-280, (1998).

[11] Wang, R. Z.H. Zhang, F., Dai, Y. J. "Parametric analysis to improve the performance of a solar desalination unit with humidifcation and dehumidification," Desalination, 142, 107-118, (2001).

[12] Soufari, S.M. Amidpour, M., Zeinali, M .A, Aghababaie, H., Zamen, M., "Experimental Investigation of a twi-stage solar humidification-dehumidification desalination process," Desalination, 332,1-6, (2014).

[13] Ben Bacha, H., Damak, T., Zhani, K., "Modeling and experimental validation of a humidification-dehumidification desalination unit solar part," Energy, 36, 3159-3169, (2011).

[14] Larson. D. C., Agarwal, V. K., "Calculation of the top loss coefficient of a flat-plate collector," Solar Energy, 27, 69-71, (1981).

[15] Boles, M. A., Cengel, Y. A., Thermodynamics an engineering approach, McGraw-Hill, (2011).

[16] Holman, J. P., Heat transfer, McGraw-Hill, 2010.